Line-Loss and Size Reduction Techniques for Millimeter-Wave RF Front-End Boards by Using a Polyimide/Alumina–Ceramic Multilayer Configuration

Masashi Nakatsugawa, *Member, IEEE,* Atsushi Kanda, *Member, IEEE,* Hiroshi Okazaki, *Associate Member, IEEE,* Kenjiro Nishikawa, *Associate Member, IEEE,* and Masahiro Muraguchi, *Member, IEEE*

***Abstract*—This paper proposes a concept for constructing low-loss and small-size millimeter-wave RF front-end boards by using a polyimide/alumina–ceramic multilayer configuration. The thick polyimide layer enables us to design low-loss wide microstrip lines (MS's). Moreover, the board size can be reduced by compactly arranging all RF and dc lines in the intermediate layers of the polyimide/alumina–ceramic substrate. The size of a prototype board designed for the quasi-millimeter-wave region is 30 mm $\times$ 30 mm. In experiments, it showed 23.2-dB linear gain and 7.4-dBm P_{-1} RF output power in transmitter (TX) mode, and 3.1-dB linear gain and $-$20.1-dBm P_{-1} IF output power in receiver (RX) mode. These performance levels agree well with predicted values. This paper further discusses applications to the integration of passive circuits fabricated in the substrate. The proposed configuration has enough potential to integrate all monolithic microwave integrated circuit (MMIC) chips, dc-bias integrated circuits (IC's), and passive circuits, and can improve the total performance in terms of the RF characteristics, board size, and fabrication cost.**

***Index Terms*—Alumina ceramic, losses, millimeter-wave technology, MMIC's, multilayer, packaging, polyimide films.**

I. Introduction

WITH THE popularization of personal communications, the demand for higher bit-rate wireless communication services is significantly increasing, and it necessitates more frequency bands than ever. For these systems, millimeter-wave frequencies are an attractive and abundant spectrum resource which allows us to employ wide-band radio communication systems. However, millimeter-wave RF technologies still need further cultivation before application to practical consumer products. The difficulties in developing millimeter-wave systems are the needs for low fabrication cost and for high-level RF performance.

For chip-size reduction and large-scale integration, three-dimensional (3-D) monolithic microwave integrated circuits (MMIC's) and masterslice technologies have been proposed [1], [2]. These technologies enable mass production of semiconductor wafers and lead to cost reduction. They adopt thin polyimide layers to form thin film microstrip lines (TFMS's). Their patterning flexibility on the semiconductor chip makes it possible to design various kinds of functional circuits and to connect them within a small area, and results in fabrication of multifunctional one-chip MMIC's [3]. Nevertheless, it is difficult to integrate circuits fabricated by different device processes into one circuit module because all unit circuits in a 3-D MMIC share the same semiconductor substrate. The ability to integrate different types of active devices improves the total circuit performance and increases the field of 3-D MMIC technology applications.

Multichip module (MCM) technologies have been focused on as one promising technique for reducing transmit/receive (T/R) module cost, as reported in high-density microwave-packaging (HDMP) program activities [4]–[7]. For cordless and cellular terminals, the use of multilayer glass epoxy boards is a good solution for minimizing their size and fabrication cost. However, their application to millimeter-wave substrates incurs difficulties because of the line-loss which increases in proportion to the frequency. Consequently, line-loss and size reduction techniques suitable for millimeter-wave RF module boards are required to build high-performance mobile terminals. In [8], electrical characteristics of MCM materials were discussed; however, no comment was made on line-loss properties of transmission lines or on the size or fabrication cost of the modules produced by MCM technologies.

In this paper, we propose a concept for reducing line loss and module size by using a polyimide/alumina–ceramic multilayer configuration. Low-loss transmission lines can be neatly patterned in the multilayered polyimide by using this configuration. DC-bias lines can be compactly arranged in the intermediate layer of the multilayered ceramic substrate. Thanks to the ground plane inserted between polyimide and ceramic layers, RF lines and dc-bias lines can be designed separately, and the interference between these lines can effectively be suppressed. All MMIC's, voltage regulators, inverters, and controller integrated circuits (IC's) are mounted on the substrate. Moreover, passive RF circuits and matching circuits for the active devices can be fabricated by low-loss transmission lines. These properties contribute to the fabrication-cost reduction because they minimize chip size by excluding

Manuscript received March 31, 1997; revised August 15, 1997.

M. Nakatsugawa is with the California Institute of Technology, Pasadena, CA 91125 USA, on leave from NTT Wireless Systems Laboratories, Yokosuka-shi, Kanagawa 239, Japan.

A. Kanda, H. Okazaki, K. Nishikawa, and M. Muraguchi are with NTT Wireless Systems Laboratories, Yokosuka-shi, Kanagawa 239, Japan.

Publisher Item Identifier S 0018-9480(97)08363-4.

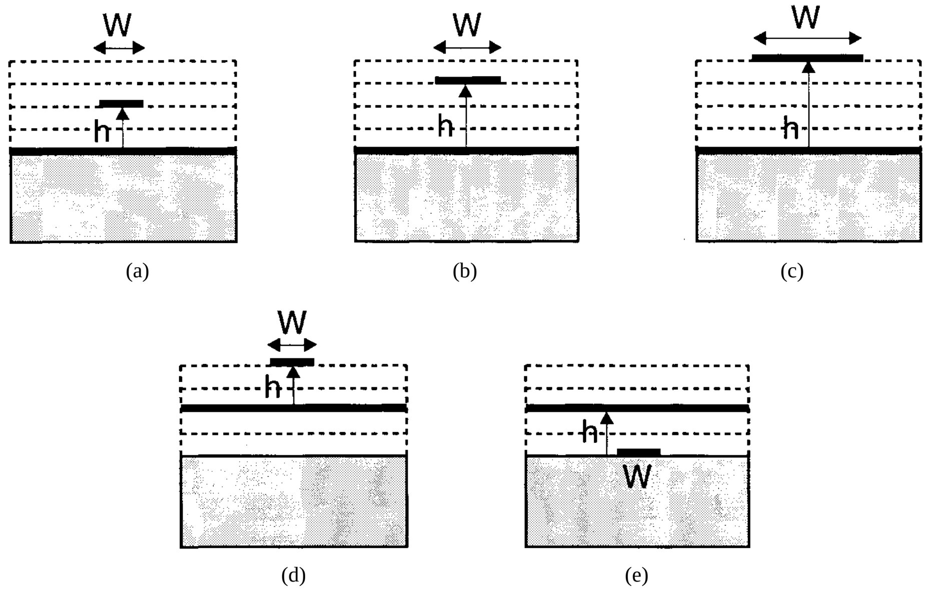

Fig. 1. Examples of a variety of wide MS's. (a) G1S3. (b) G1S4. (c) G1S5. (d) G3S5. (e) G3S1.

TABLE I
COMPARISON OF MULTILAYER SUBSTRATE MATERIALS

	PI/ceramic	Alumina	Glass Epoxy
Cost	Good	Good	Excellent
RF performance (>10 GHz)	Good	Excellent	Poor
Size	Excellent	Fair	Good
Fine pattern	Good	Fair	Good
Easy fabrication	Fair	Fair	Excellent

TABLE II
DIMENSIONS OF WIDE MS'S

	h (μm)	W (μm)
G1S3	50	88
G1S4	75	150
G1S5	100	220
G3S5	50	100
G3S1	50	50

passive circuit areas, which occupy most parts of MMIC's. This configuration is successfully applied to the RF module board for the quasi-millimeter-wave region.

II. PROPERTIES OF POLYIMIDE/ALUMINA–CERAMIC

A. Material Comparison

Glass epoxy and alumina ceramic are often used for the RF boards. We compared the properties of polyimide/alumina–ceramic with those of glass epoxy and alumina ceramic. The results are summarized in Table I.

Glass epoxy is superior to other materials in terms of cost and ease of fabrication. This is the reason that glass epoxy substrate is now widely adopted for many kinds of RF boards. However, its RF performance degrades with an increase in frequency because of its large loss tangent [8]. Therefore, it is difficult to apply this substrate to RF boards for the millimeter-wave range.

When the transmission lines are formed on the alumina surface, they show excellent performance even in the millimeter-wave region thanks to the small loss tangent. Despite this performance, they have drawbacks in size reduction and fine patterning for RF lines. Multilayer alumina substrates are usually produced by a co-fired process. Because lines inside the ceramic substrate are patterned with screen printing techniques, their resolution is coarser than that of photolithography. Moreover, these lines need to be made from cermets. Since they have higher sheet resistance than the pure metals plated on the surface, only the lines on the surface of the substrate are available for the low-loss RF lines at high-frequency region. This causes limitations in pattern layout.

Polyimide/alumina–ceramic inherits advantages from multilayer alumina substrates, and can effectively combine these with the advantages of a multilayer polyimide structure. Since all transmission lines in multilayer polyimide can be fabricated by photolithography, low line-loss and fine patterning become possible. In addition, other lines for dc biases can be fabricated in the multilayer alumina–ceramic.

B. RF Performance of Wide Microstrip Lines

Fig. 1 shows examples of a variety of wide microstrip lines (MS's) which can be fabricated in the proposed polyimide/alumina–ceramic configuration. Metal layers are indicated as thick solid lines. The dimensions for these wide MS's are shown in Table II. They are distinguished by names of the form $GnSm$, where n is the number for the ground plane and m is for metal layer. These numbers are counted from bottom to top layer. The thickness of each polyimide is 25 μm. The

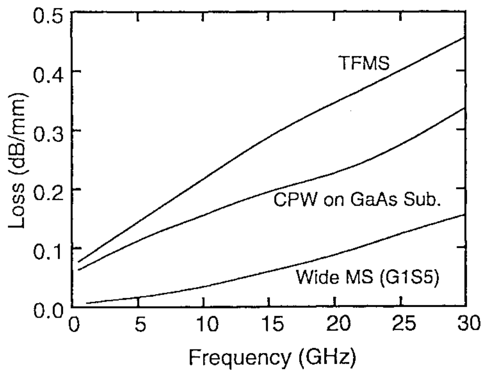

Fig. 2. Loss comparison between wide MS, CPW, and TFMS.

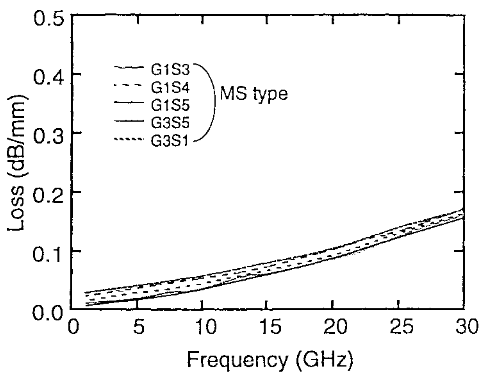

Fig. 3. Loss comparison: various types of wide MS's.

loss of the wide MS line ($G1S5$) was measured and compared with that of coplanar waveguide (CPW) on GaAs substrate and TFMS (Fig. 2). The losses at 20 GHz for wide MS, TFMS, and CPW are 0.083, 0.34, and 0.22 dB/mm, respectively. The wide MS has approximately 1/4 the loss of the TFMS, and this result shows its suitability for use as RF lines and passive circuits. Fig. 3 shows the loss comparison between wide MS's shown in Fig. 1. All of these losses are better than CPW on GaAs substrate, and they show quite low-loss performance.

Measured results for the effective dielectric constant and characteristic impedance of wide MS ($G1S5$) are shown in Figs. 4 and 5. Flat characteristics were obtained over the frequency range from 1 to 30 GHz. These results confirm that they are usable over this frequency range.

III. Configuration

A. Multilayer Polyimide/Alumina–Ceramic Board

The methods considered, for achieving low-loss and small-size boards with a polyimide/alumina–ceramic multilayer configuration are: 1) line loss reduction by using wide MS's; 2) size reduction by mounting all IC's on the surface of the substrate and by arranging all lines three dimensionally; and 3) circuit stabilization by using metal–insulator–metal (MIM) capacitors fabricated on the ceramic substrate [9].

An example of the proposed configuration is shown in Fig. 6(a) and (b). The board consists of four 25-μm-thick polyimide layers and four 250-μm-thick ceramic layers [10]. The metal used in the polyimide layer is 5-μm-thick copper,

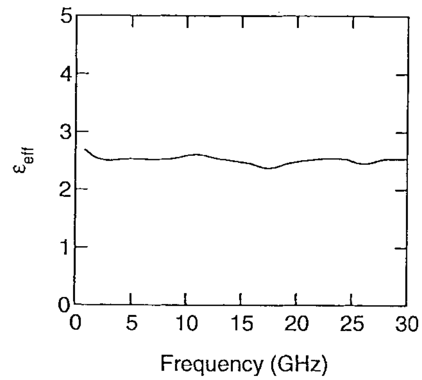

Fig. 4. Measured effective dielectric constant versus frequency.

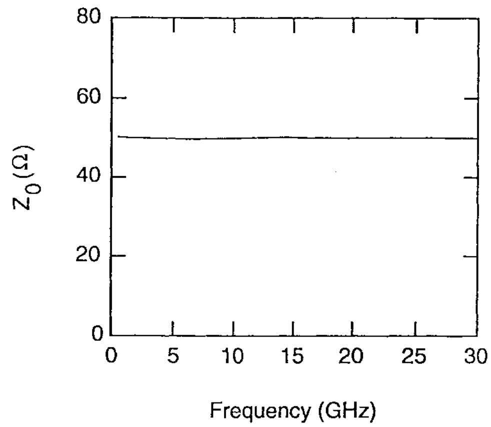

Fig. 5. Characteristic impedance versus frequency.

and in the ceramic layer is tungsten. Between polyimide and ceramic layers, a ground plane is inserted to form the ground for RF lines and to avoid interference between RF and dc-bias lines. Owing to this ground plane, the transmission lines for RF signals and dc-bias lines can be designed separately. MIM capacitors are also fabricated on this surface.

The polyimide layer is thick enough to allow the design of wider MS's (linewidth >50 μm) than TFMS's (linewidth 10–30 μm). The wide MS's are used as the RF signal lines for MMIC's. Lines are sufficiently isolated from each other at high frequency when spacing is at least three times as much as the substrate thickness [2]. The multilayer ceramic substrate holds the MMIC's on the polyimide-side surface, while on the ceramic-side are other IC's for the dc biases, such as voltage regulators, dc–dc converters, RF-switch controllers, etc. Rectangular areas of the polyimide layer were removed to open the mounting areas for MMIC's. The MMIC's were then mounted on the ceramic surface with conductive paste. The thickness of these MMIC's was thinned to between 100–150 μm to adjust their height to be close to that of the polyimide surface. The dc-bias lines were formed on the ceramic surface or inside the ceramic substrate. One end of each dc-bias line was connected to the IC's for the dc biases at the ceramic surface. The other end was drawn to the top polyimide surface through a via-hole to be connected to the bias/control pads of the MMIC's. In order to stabilize

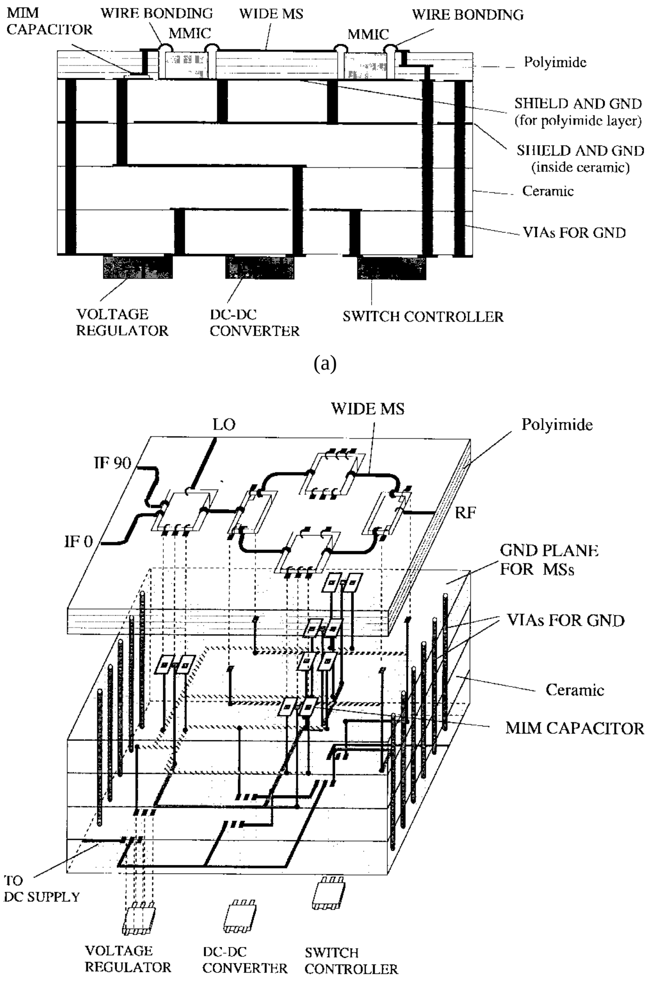

Fig. 6. An example of proposed configuration (a) cross section and (b) overview.

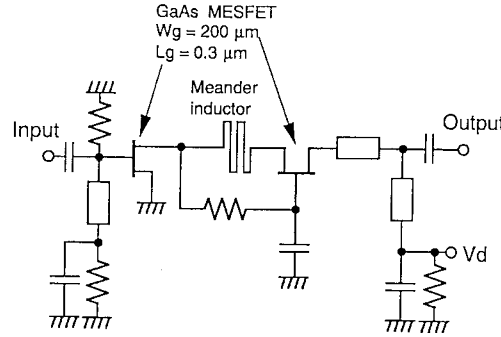

Fig. 7. Schematic circuit of the type-B buffer amplifier.

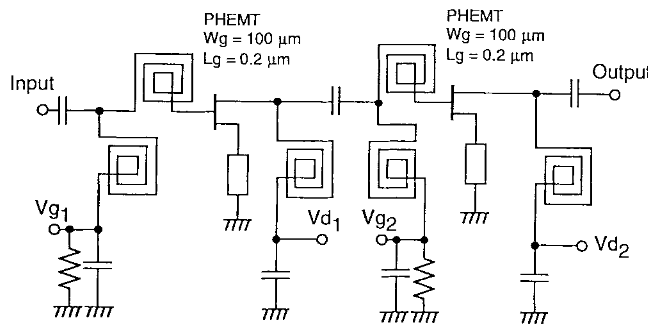

Fig. 8. Schematic circuit of the PHEMT LNA.

circuit operation and to eliminate parasitic oscillation, MIM capacitors were formed on the alumina substrate surface, and they were connected to the dc-bias lines as bypass capacitors. All lines were bonded to the MMIC's with 20-μm gold wires. RF lines were especially tightly connected with some minimal-length wires. The MS lines are converted to CPW's at the points where MMIC pads are bonded to wide MS's so as to be measured with on-wafer probing systems. Thus, performances before and after mounting MMIC chips are easily scrutinized with these structures.

B. RF MMIC Chips

We constructed an RF board with some prototype MMIC chips, which are used to verify the board performance. A low-noise amplifier, an RF switch, and a T/R mixer were newly designed for this board, and all MMIC chips were designed for the 19-GHz band.

The transmitter (TX) branch is composed of three GaAs MESFET buffer amplifiers and a pseudomorphic high electron-mobility transistor (PHEMT) TX amplifier. Two types of buffer amplifier were designed. Type-A is a two-stage common-source amplifier adopting two GaAs MESFET's, each with a 100-μm gatewidth and a 0.3-μm gate length. Transmission lines were used for the matching circuits. The chip size of the type-A buffer amplifier is 1.8 mm $\times$ 1.3 mm. Fig. 7 shows the schematic circuit of the type-B buffer amplifier, which adopts two GaAs MESFET's, each with a 200-μm gatewidth and a 0.3-μm gate length. In order to attain high gain with small chip size, this circuit employs a cascode FET with additional inductance [11], [12]. A meander inductor was used for this inductance. The chip size of the type-B buffer amplifier is 0.8 mm $\times$ 0.8 mm. The PHEMT TX amplifier was a commercially available MMIC (HMMC5618) produced by Hewlett-Packard.[1]

The receiver (RX) branch is composed of a PHEMT low noise amplifier (LNA) and a type-A buffer amplifier. The PHEMT LNA was designed for the first block amplifier in the RX branch. Its schematic circuit is shown in Fig. 8. Two PHEMT's, each of whose gatewidth is 100 μm and gate length is 0.2 μm, were used in this LNA. The input stage was designed for low noise matching and the output-stage part for high gain matching. All matching circuits were composed of spiral inductors to reduce chip size. Parasitic elements in these inductors were carefully considered through the circuit design process. The chip size of this LNA is 0.88 mm $\times$ 0.88 mm.

The mixer is a subharmonically pumped image-rejection SSB mixer using antiparallel diodes [13], [14]. Since this one is a passive mixer, it can be used for an up and down converter (DC). Fig. 9 shows the schematic circuit of the mixer. In order to minimize chip size, a Wilkinson divider and a quadrature hybrid were designed by lumped-element techniques [15]. Capacitors C_{RF} and C_{LO} are used to prevent

[1] *GaAs Integrated Circuits, Data Sheets and Family Summaries,* Hewlett-Packard Co., pp. 2-27–2-32.

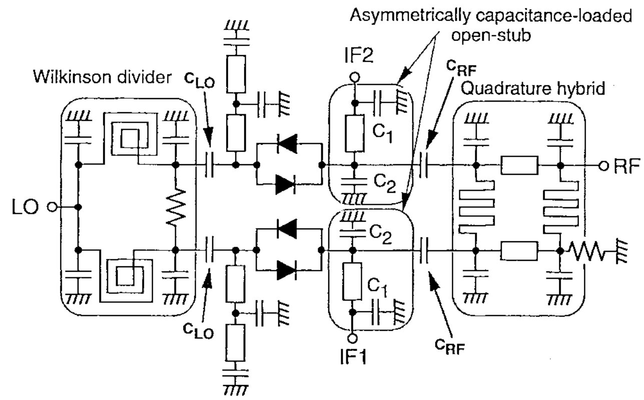

Fig. 9. Schematic circuit of the image-rejection single sideband (SSB) mixer.

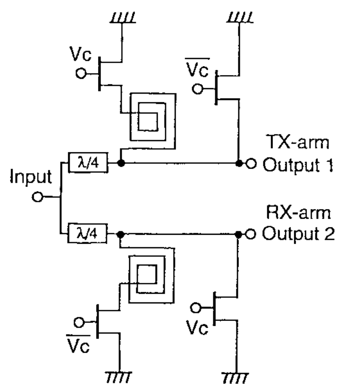

Fig. 10. Schematic circuit of the SPDT RF switch.

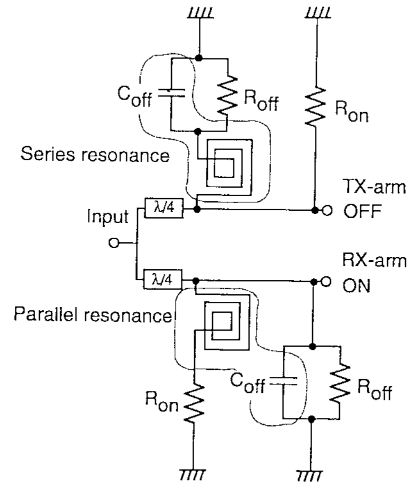

Fig. 11. Simplified equivalent circuit of the SPDT RF switch.

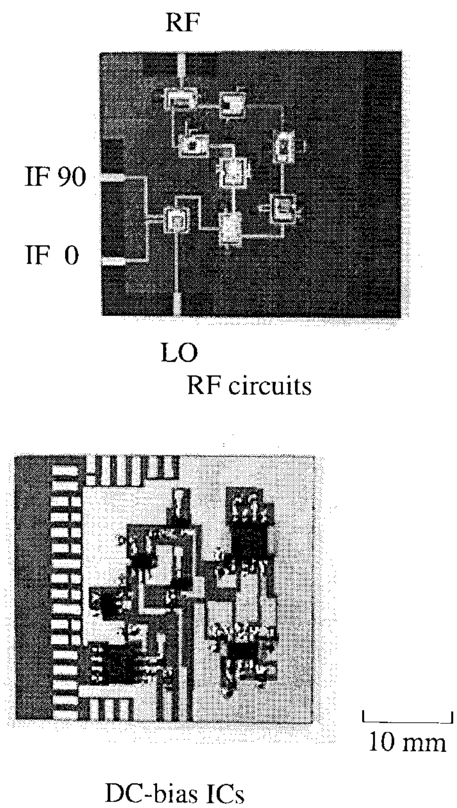

Fig. 12. Photographs of the prototype RF board.

IF signal injection toward LO and RF ports. Asymmetrically capacitance-loaded open-stubs, which have the same characteristics of quarter-wavelength stub at fundamental and second harmonic frequency, were newly designed. The stub was used as a filter to suppress the LO level and to obtain 2LO signals. Loaded capacitances, C_1 and C_2, are calculated as

$$C_1 = 1/(2\pi \times f_{\mathrm{LO}} \times Z \times \tan\theta)$$
$$C_2 = C_1/(3 + \tan^2\theta)$$

where, f_{LO} is local frequency for the mixer, and θ is electrical length of the transmission line at f_{LO}. In order to omit low-pass filters for IF signals, an IF port was placed at the point where the shunt capacitor and the transmission line are connected in this asymmetrical stub. The chip size of the mixer is 1.28 mm $\times$ 1.28 mm.

A GaAs FET-based single-pole double-throw (SPDT) switch was used for a T/R switch. In the high-frequency region, the off-state FET's impedance becomes low because of its parasitic capacitance, and it degrades both isolation performance between TX/RX arms and insertion loss performance of the on-state arm. In order to eliminate this effect, the *LC* series resonant circuit was employed. Fig. 10 shows the schematic circuit of the SPDT switch. The simplified equivalent circuit is shown in Fig. 11. In this figure, the on-state FET is drawn as the resistor R_{on} and off-state FET is drawn as a combination of the capacitor C_{off} and the resistor R_{off}, which are connected in parallel. An inductor, whose inductance was chosen so as to resonate with C_{off}, is connected to the FET. An additional shunt FET switch is connected to both TX and RX arms. On the off-state arms (upper arm in Fig. 11), the inductor and C_{off} resonate in series at the designated frequency. Since the impedance of this part becomes very small, the impedance seen from the input port is almost infinity and that seen from the off-state output port is "short." These properties can improve isolation performance of the switch. The on-state shunt switch also improves isolation performance. On the on-state arms (lower arm in Fig. 11), the inductor and C_{off} in shunt FET

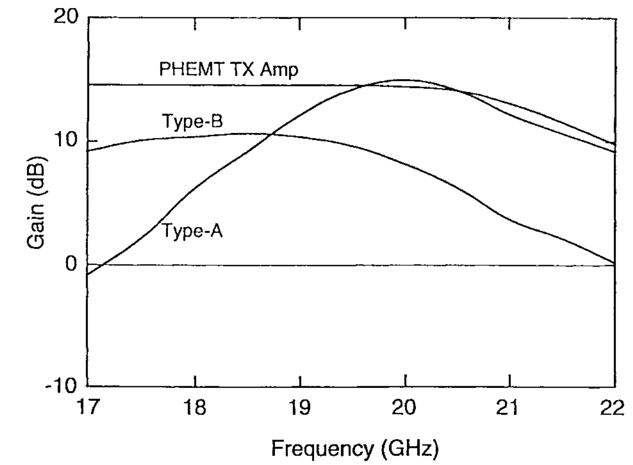

Fig. 13. Gains of type-A, type-B, and PHEMT TX amplifiers.

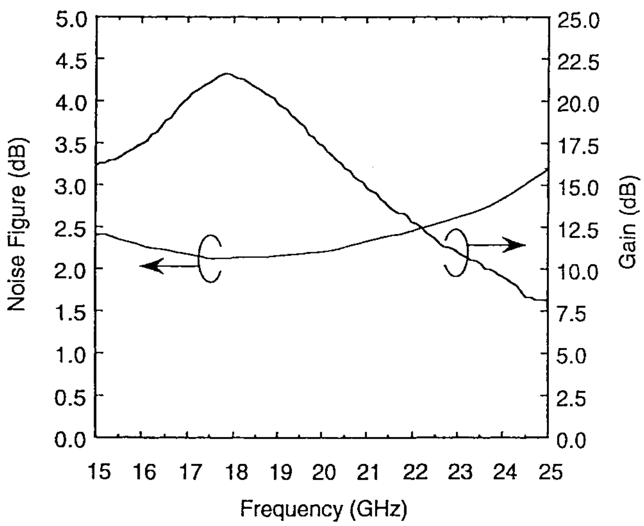

Fig. 14. Gain and NF of the PHEMT LNA.

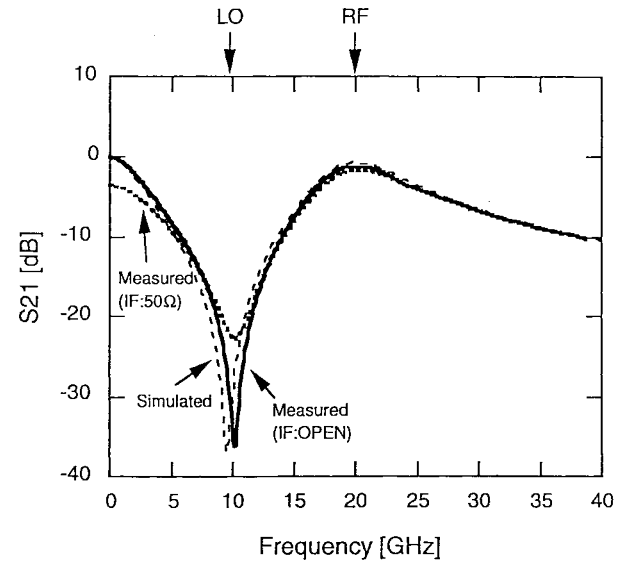

Fig. 15. Characteristics of asymmetrically capacitance-loaded open-stub.

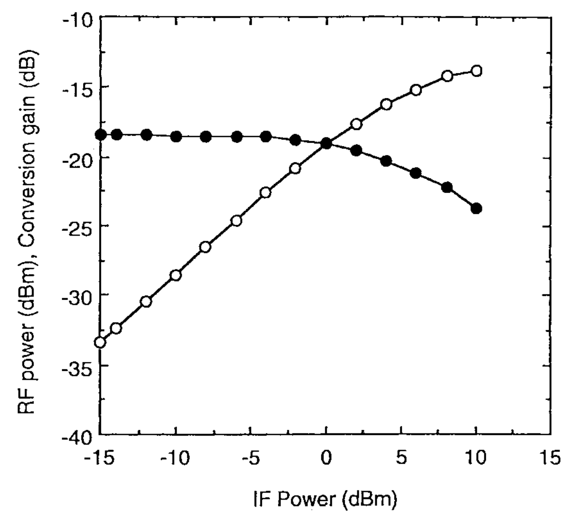

Fig. 16. RF power and conversion gain of the mixer (UC).

switch resonate in parallel at the designated frequency. The total impedance of the circuits connected to the off-state arm becomes infinity, and the insertion loss of the on-state arm can be made very small.

IV. Results and Discussions

Fig. 12 shows the photographs of the prototype RF board, seen from the RF circuit surface (polyimide surface) and the dc-bias IC surface (ceramic surface). Nine MMIC chips are mounted on the polyimide surface. On the ceramic surface, five dc-bias IC's, some chip-resistors, and chip capacitors are soldered. The area occupied by these chips is 30 mm $\times$ 30 mm, excluding the dc connector area. The size of this module can be reduced to 25 mm $\times$ 25 mm by cutting off the design margin space.

The performance of each MMIC and overall performance were measured. Drain bias voltage for all MMIC amplifiers is 3 V. As shown in Fig. 13, the gains of type-A, type-B, and PHEMT TX amplifiers are 14.0, 8.9, and 14.3 dB at 19.5 GHz, respectively. The obtained gain performances are almost the same as those of the simulation. Gain and noise figure (NF) performance of the PHEMT LNA is shown in Fig. 14. At 19.5 GHz, gain and NF are 16.8 and 2.2 dB, respectively. The characteristics of the asymmetrically capacitance-loaded open-stub are shown in Fig. 15. Sufficient suppression at LO frequency and small insertion loss at 2LO frequency were obtained, and they agree with simulated results. The performance with IF port terminated was also measured. It was almost equal to the case without termination, and this result exhibits that this IF port can be used to omit low-pass filters. The mixer's conversion gains and output powers, as an up converter (UC) and a DC, are shown in Figs. 16 and 17. The injected LO power was 9 dBm and its frequency was 9.6925 GHz. IF was chosen as 140 MHz. As an up converter, it has a conversion gain of 18.4 dB at input power of -15 dBm. As a DC, 18.1-dB conversion gain is obtained at input power of -10 dBm. Image rejection ratio was 18.0 dB. Insertion loss and isolation performances of the RF switch are shown in Fig. 18. It exhibits 1.9-dB insertion loss and 20.0-dB isolation at 19.5 GHz.

The performance of the board was measured in TX and RX modes. The injected LO power was 9 dBm and its fre-

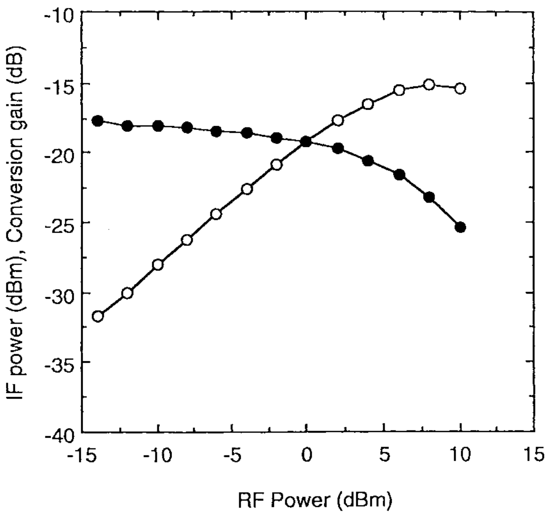

Fig. 17. IF power and conversion gain of the mixer (DC).

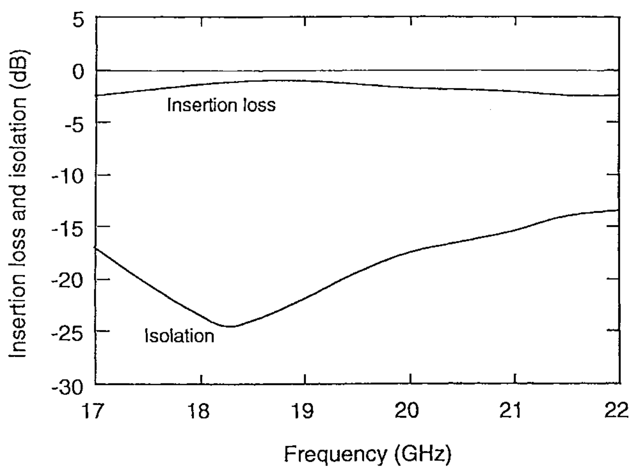

Fig. 18. Insertion loss and isolation of the SPDT switch.

quency was 9.6925 GHz, which was subharmonically doubled and mixed in the mixer. IF was chosen as 140 MHz. The performance of the board in TX mode is shown in Fig. 19. It shows 23.2-dB gain and 7.4-dBm P_{-1} output power. The performance of the board in RX mode is shown in Fig. 20. It shows 3.1-dB gain, and -20.1-dBm P_{-1} output power. When these performance measurements were made, there was no parasitic oscillation.

The overall performance of the board, obtained through experiments, agreed well with the predicted overall performance. The transmission loss is sufficiently low, and all MMIC's and dc-bias IC's operate without difficulties. These experimental results confirm the validity of the proposed configuration, which is applicable to millimeter-wave RF module boards.

In the prototype board, the polyimide layer is used only for connecting MMIC chips. The multilayer polyimide structure has advantages in the fabrication of some kinds of passive circuits, such as broadside couplers [16], filters [17], and power dividers/combiners [1]. Fig. 21 shows an example of passive circuit integration. By using bump bonding technologies, the loss performance at the connection between semiconductor chips and transmission lines can be improved. Since relatively large RF passive components can be fabricated in the substrates by using low-loss MS's, we can minimize MMIC chip size. The proposed configuration has enough potential to integrate these passive circuits with MMIC chips and can improve the total performance in terms of the RF characteristics, board size, and fabrication cost.

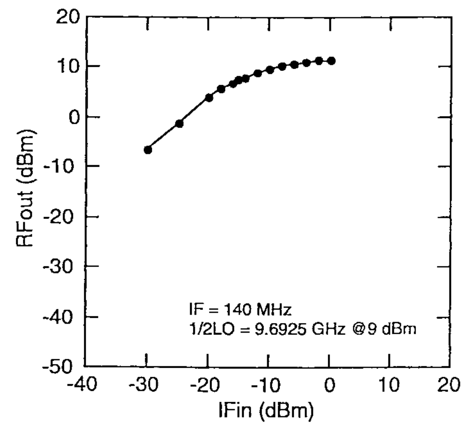

Fig. 19. Performance of the board: TX mode.

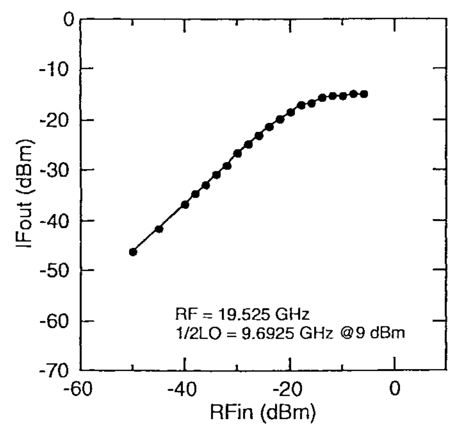

Fig. 20. Performance of the board: RX mode.

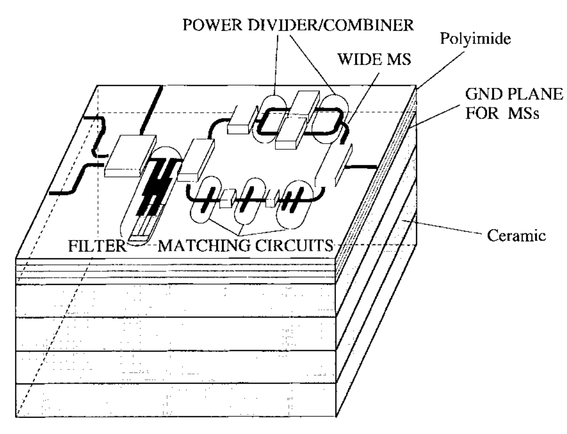

Fig. 21. An example of passive circuit integration.

V. Conclusion

A multilayer polyimide/alumina–ceramic substrate was successfully applied to quasi-millimeter-wave band modules. The low-loss performance of the wide MS's exhibits their suitability for use even in the millimeter-wave region. The 3-D line layout contributes to module size reduction. These results are promising for realizing millimeter-wave module boards. These modules are suitable for application as RF boards in millimeter-wave mobile terminals.

ACKNOWLEDGMENT

The authors would like to thank A. Hashimoto and Dr. M. Aikawa for their fruitful discussions and encouragement through this work. They would also like to thank K. Maruyama of NTT Electronics Technology Corporation for his excellent technical support.

REFERENCES

[1] T. Tokumitsu, T. Hiraoka, H. Nakamoto, and M. Aikawa, "Multilayer MMIC using a 3 μm × N-layer dielectric film structure," *IEICE Trans. Electron.*, vol. E75-C, no. 6, pp. 698–706, June 1992.
[2] T. Tokumitsu, K. Nishikawa, K. Kamogawa, I. Toyoda, and M. Aikawa, "Three-dimensional MMIC technology for multifunction integration and its possible application to masterslice MMIC," in *IEEE Microwave Millimeter-Wave Monolithic Circuits Symp. Dig.*, San Francisco, CA, June 1996, pp. 85–88.
[3] M. Aikawa, T. Tokumitsu, and K. Nishikawa, "Advanced MMIC technology for the next generation-3D MMIC's and master-slice technology," in *Proc. 26th European Microwave Conf.*, Prague, Czech Republic, Sept. 1996, pp. 748–753.
[4] E. D. Cohen, "High density microwave packaging program," in *IEEE Int. Microwave Symp. Dig.*, Orlando, FL, May 1995, pp. 169–172.
[5] J. A. Reddick, III, R. K. Peterson, M. Lang, W. R. Kritzler, P. Piacente, and W. P. Kornrumpf, "High density microwave packaging program phase 1—Texas Instruments/Martin Marietta team," in *IEEE Int. Microwave Symp. Dig.*, Orlando, FL, May 1995, pp. 173–176.
[6] J. A. Costello, K. Kline, F. Kuss, W. Marsh, R. Kam, B. Fasano, M. Berry, and N. Koopman, "The Westinghouse high density microwave packaging program," in *IEEE Int. Microwave Symp. Dig.*, Orlando, FL, May 1995, pp. 177–180.
[7] J. Wooldridge, "High density microwave packaging for T/R modules," in *IEEE Int. Microwave Symp. Dig.*, Orlando, FL, May 1995, pp. 181–184.
[8] S. Riad, W. Su, A. Elshabini-Riad, F. Barlow, and I. Salama, "Wideband electrical characterization of MCM materials," *Electron. Package. Prod.*, pp. 47–52, June 1996.
[9] R. Kambe, R. Imai, T. Takada, M. Arakawa, and M. Kuroda, "MCM substrate with high capacitance," *IEEE Trans. Comp., Packag., Manufact. Technol. B*, vol. 18, pp. 23–27, Feb. 1995.
[10] K. Kamogawa, T. Tokumitsu, and M. Aikawa, "Multifrequency microstrip antennas using alumina-ceramic/polyimide multilayer dielectric substrate," *IEEE Trans. Microwave Theory Tech.*, vol. 44, pp. 2431–2437, Dec. 1996.
[11] T. Hirota, "A Ka-band small-size monolithic amplifier," in *IEICE Spring Nat. Conv. Rec.*, (in Japanese), Tokyo, Japan, Mar. 1990, pt. 2, p. 477.
[12] I. Toyoda, T. Tokumitsu, and M. Aikawa, "Highly integrated three-dimensional MMIC single-chip receiver and transmitter," *IEEE Trans. Microwave Theory Tech.*, vol. 44, pp. 2340–2346, Dec. 1996.
[13] M. Cohn, J. E. Degenford, and B. A. Newman, "Harmonic mixing with an antiparallel diode pair," *IEEE Trans. Microwave Theory Tech.*, vol. MTT-23, pp. 667–673, Aug. 1975.
[14] H. Okazaki and Y. Yamaguchi, "SSB subharmonically pumped mixer MMIC for a 20 GHz-band transceiver," (in Japanese), IEICE, Tech. Rep. MW96-42, OPE96-22, pp. 13–18, June 1996,.
[15] T. Hirota, A. Minakawa, and M. Muraguchi, "Reduced-size branch-line and rat-race hybrids for uniplanar MMIC's," *IEEE Trans. Microwave Theory Tech.*, vol. 38, pp. 270–275, Mar. 1990.
[16] I. Toyoda, T. Hirota, T. Hiraoka, and T. Tokumitsu, "Multilayer MMIC branch-line coupler and broad-side coupler," in *IEEE Microwave Millimeter-Wave Monolithic Circuits Symp. Dig.*, Albuquerque, NM, June 1992, pp. 79–82.
[17] I. Toyoda, T. Tokumitsu, and K. Nishikawa, "A multilayer MMIC filter using short-line meshes (SLM's)," in *Proc. 24th European Microwave Conf.*, Cannes, France, Sept. 1994, pp. 443–447.

Masashi Nakatsugawa (M'93) was born in Hamamatsu, Japan, in 1963. He received the B.E. degree in electronics and communication engineering and the M.E. degree in electrical engineering from Waseda University, Tokyo, Japan, in 1987 and 1989, respectively.

In 1989, he joined NTT Radio Communication Systems Laboratories, Yokosuka, Japan, where he has been involved in research on MMIC's. He was a Research Engineer at NTT Wireless Systems Laboratories, Yokosuka, Japan, where he was engaged in the development of microwave amplifiers, control circuits, and packaging technologies. He is currently on leave from NTT, studying at the California Institute of Technology, Pasadena

Mr. Nakatsugawa was the recipient of the 1996 Young Engineer Award given by the Information and Communication Engineers (IEICE), Japan. He is a member of the IEICE and the Japan Society of Applied Physics.

Atsushi Kanda (M'95), for a photograph and biography, see this issue, p. 2233.

Hiroshi Okazaki (A'94) was born in Okayama, Japan, in 1965. He received the B.E. and M.E. degrees from Osaka University, Osaka, Japan, in 1988 and 1990, respectively.

In 1990, he joined NTT Radio Communication Systems Laboratories, Yokosuka, Japan, and has been involved in the investigation of low power-consumption SSPA's for earth stations. He is currently a Research Engineer at NTT Wireless Systems Laboratories, Yokosuka, Japan, where he is engaged in research on microwave-circuit techniques for monolithic integration.

Mr. Okazaki was the recipient of the 1997 Young Engineer Award given by the Institute of Electronics, Information, and Communication Engineers (IEICE), Japan.

Kenjiro Nishikawa (A'93) was born in Nara, Japan, on September 18, 1965. He received the B.E. and M.E. degrees in welding engineering from Osaka University, Suita, Japan, in 1989 and 1991, respectively.

In 1991, he joined the NTT Radio Communication Systems Laboratories (now NTT Wireless Systems Laboratories), Yokosuka, Japan. He has been engaged in research and development on 3-D and uniplanar MMIC's on Si and GaAs, and their applications.

Mr. Nishikawa was the recipient of the 1996 Young Engineer Award by the Institute of Electronics, Information, and Communication Engineers (IEICE), Japan. He is a member of the IEICE.

Masahiro Muraguchi (S'81–M'81) was born in Kanazawa, Japan, in 1955. He received the B.S. degree in electrical engineering from the Nagoya Institute of Technology, Japan, in 1978, and the M.S. and Ph.D. degrees in physical electronics engineering from the Tokyo Institute of Technology, Tokyo, Japan, in 1980 and 1983, respectively.

In 1983, he joined the NTT Atsugi Electrical Communications Laboratories, Nippon Telegraph and Telephone Corporation, where he was involved in the design and fabrication of GaAs MMIC's. He is currently engaged in research and development work on MMIC's for wireless communications at the NTT Wireless Systems Laboratories, Yokosuka, Japan, where he is the Leader of the Microwave Circuit Group.

Dr. Muraguchi is a member of the Institute of Electronics, Information, and Communication Engineers (IEICE), Japan. Since 1994, he has been on the editorial committee of *IEICE Transactions on Electronics* as an associate editor. He was awarded the Ichimura Prize by the New Technology Development Foundation in 1994.